ICRC 2001

The hybrid aperture and precision of the Auger observatory

B. Dawson[1] **and P. Sommers**[2], **for the Pierre Auger Collaboration**[3]

[1]Physics Department, University of Adelaide, Adelaide SA 5005, Australia
[2]Physics Department, University of Utah, Salt Lake City UT 84112 USA
[3]Observatorio Pierre Auger, Av. San Martin Norte 304, (5613) Malargüe, Argentina

Abstract. The Pierre Auger Observatory has been designed as a hybrid detector, taking advantage of complementary observational techniques - a surface array of water Cherenkov detectors coupled with four air fluorescence detector sites. Such a combination provides excellent reconstruction of the shower axis geometry using information from both the fluorescence and surface detectors, even at energies below the nominal detector threshold of 10^{19}eV. It also allows for powerful cross-checks of detector performance and analysis techniques through the comparison of surface-only and fluorescence only reconstruction of the same showers. In this paper we describe the motivation for building a hybrid detector, and we outline the hybrid reconstruction technique. The hybrid aperture as a function of energy is presented, together with expected resolution figures for shower geometry, energy and the depth of shower maximum.

1 Introduction

The Pierre Auger Project's southern site near Malargüe, Argentina is under construction (Dova, 2001). Three thousand square kilometres of land area will be covered by an array of 1600 10m^2 water Cherenkov detectors on a 1.5 km triangular grid. Four air fluorescence (Fly's Eye-type) detectors will monitor the atmosphere above the array.

An array of water Cherenkov detectors and a fluorescence eye have complementary strengths capable of thoroughly characterizing the nature of an extensive air shower. The fluorescence detector (FD) records energy deposition in the atmosphere and provides a measurement of the charged particle longitudinal profile. A snapshot of the shower front is captured by the surface detectors (SD) at ground level, at a depth where particle densities at large core distances are near their maximum values.

Fluorescence detectors can only operate on clear moonless

Correspondence to: B. Dawson
(bdawson@physics.adelaide.edu.au)

nights, and experience shows that this will limit their duty cycle to approximately 10%. But during this time Auger's hybrid combination of fluorescence and surface detectors can provide superior resolution in arrival directions, energies and mass to that expected from the surface array or a single eye alone.

2 Benefits of a Hybrid System

The hybrid concept was born from a desire to design an observatory that could provide reliable and believable measurements of the the highest energy cosmic rays (Sommers, 1995; Dawson et al., 1996). The Auger water Cherenkov detectors are relatively simple and robust, and use long established methods for estimating arrival directions and energy. They also offer promising mass composition discrimination. The 100% duty cycle available with the SD is attractive, but our collaboration thought it unwise to construct the Auger observatory with a ground array alone. The fluorescence detectors are a vital part of the design, for several reasons.

Firstly, the fluorescence detectors will provide valuable cross checks for many of the measurements made by the surface detectors. The two detector types aim to measure the same properties of primary cosmic rays (energies, mass composition, etc.) but do so using different techniques with *very different systematics*. Thus the fluorescence detectors serve to cross-check and train the surface array, providing confidence in the array results for the 90% of the time when no fluorescence detector is operating.
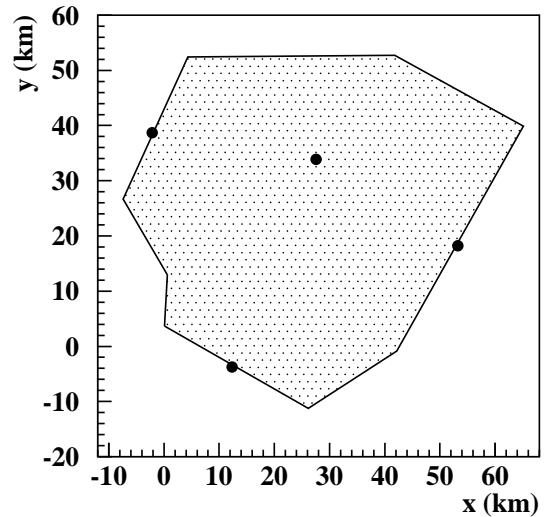
However, the fluorescence detectors are much more than calibration tools. The data set collected during the 10% of time that the Hybrid is operating will be of the highest quality, being especially useful for those studies that require more precise shower directions and studies where longitudinal profile measurements are vital.

An example of an important cross-check is in the area of energy assignment. The SD determines primary energy from estimates of the water Cherenkov detector density 1000 m

from the shower core. This is a modification of the Haverah Park technique which used a core distance of 600 m. The technique uses the fact (borne out in simulations) that at these energies the density at large core distances is insensitive to development fluctuations, and is a measure of primary energy. The conversion factors must come from air shower simulations, and this is where comparisons with fluorescence measurement become important. The fluorescence technique uses the atmosphere as a giant calorimeter, where energy deposition is measured via the nitrogen fluorescence light it induces (Cester, 2001). The FD measurement of energy is therefore model independent. Atmospheric variability (mostly changing aerosol properties) complicates the analysis, however, due to essential correction for atmospheric attenuation of the fluorescence light and also correction for contamination of the signal by scattered Cherenkov light. The appropriate corrections must be based on atmospheric monitoring at the observatory. The SD and FD therefore have very different systematics in their measurement of energy, and a comparison of measurements on a set of showers will be valuable in understanding the strengths and limitations of each technique. It may be that the FD can best train the SD with showers that land relatively close to the FD sites, while the SD provides a valuable check on the FD atmospheric corrections for showers that land far from any FD site. Hybrid shower analysis benefits from the calorimetry of the FD technique and the from the uniformity of the SD aperture.


Fig. 1. The planned arrangement of detectors at the southern Auger site. The small dots represent approximate positions for the 1600 surface detectors, with the large dots indicating the fluorescence stations. The perimeter fluorescence sites are located (clockwise from bottom) at Los Leones, Coihueco and Morados, and each views a 180° range of azimuth. The central site is occupied by a detector viewing the full azimuth range. The origin of the coordinate system is the Auger data collection center in the town of Malargüe.

3 The Southern Auger Site

The choice of the number and location of fluorescence sites within the surface array was driven by the desire to minimize the effects of atmospheric uncertainties on reconstruction. The arrangement is shown in Figure 1 with one full-azimuth station near the center of the array, and three stations on the perimeter that look inward with 180° of azimuth. Each eye views elevation angles up to approximately 30°. With this arrangement, the mean impact parameter from the closest triggering station for 10^{19}eV showers is 13 km, compared with an effective Rayleigh scattering attenuation length of 19.5 km at 350 nm (averaged over all light paths). This reduces the uncertainty in atmospheric transmission corrections, while at the same allowing a relaxed design for individual telescopes that are not required to detect showers at great distances. Compared with a design using a single far-sighted eye, the four station model allows us to build less expensive telescopes with smaller mirrors and fewer pixels per telescope. The overall cost is close to the cost of the single eye design, even allowing for the extra site preparation costs, and we reduce the atmospheric uncertainties in the shower reconstruction analysis.

4 Hybrid Reconstruction of the Shower Axis

Good determination of the shower axis is the first step towards good energy and mass composition assignments. We have developed a reconstruction technique which uses FD pixel timing and amplitude information from a single eye, together with timing information from the SD, to estimate the position of the shower axis in space with excellent precision (Sommers, 1995; Dawson et al., 1996). The precision is comparable to that achieved with "stereo" fluorescence views of air showers.

Briefly, this method first uses signal strengths in triggered eye pixels to define what is known as the shower-detector plane, that plane in space containing the shower axis and a point representing the detector. The normal vector to this plane can be determined with a precision of about 0.25°. To determine the position of the axis within this plane, we use light arrival times in each pixel. Essentially, we need to measure the angular velocity ω of the shower front as seen by the eye, and its time-derivative $\dot{\omega}$. The former is much easier to measure than the latter, especially for shower tracks that subtend only a small angle, with uncertainty in $\dot{\omega}$ leading to a degeneracy in solutions to the track geometry within the plane (see Figure 2). This impasse can be broken by using additional information from the SD, in particular the arrival times of the shower front at the ground. All SD stations and the FD sites will be equipped with GPS clocks, giving timing
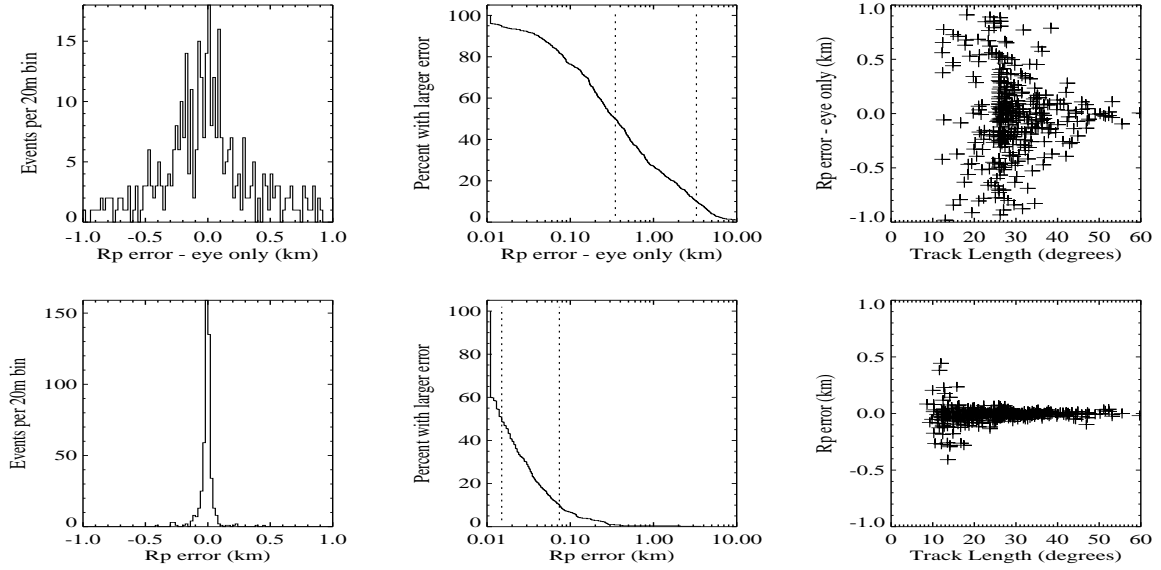
Fig. 3. Comparing fluorescence-only and hybrid reconstruction of the shower axis within the shower-detector plane, for showers of energy 10^{19}eV landing at random positions within the array. The plots in the top row show the expected reconstruction precision for the impact parameter R_p using information from a single eye only. The precision is poor, with a strong dependence on track length, the angular extent of the event. The same sample of events is then reconstructed using the hybrid method, including timing information from the SD (second row). The extra information dramatically improves the resolution. The central plot in both rows shows the integral R_p error distribution, with the median and 90% error values indicated with vertical dashed lines.
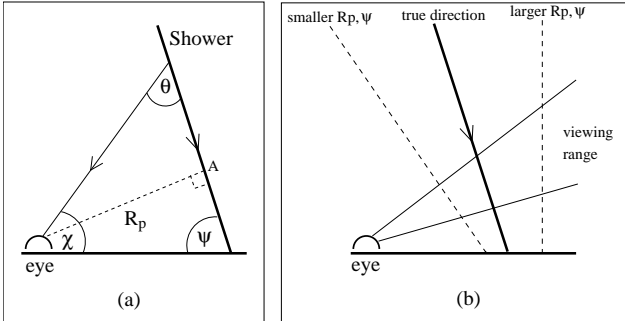
Fig. 2. (a) Geometric reconstruction within the shower-detector plane. A phototube views the shower axis at an angle θ to the shower axis. (b) A highly exaggerated illustration of the ambiguity in the reconstruction when the track length viewed by the FD is small. The dashed lines show alternative solutions which exhibit source angular velocities ω similar to that of the true geometry. The ambiguity can be lessened by a measurement of $\dot{\omega}$ (easiest with a longer track-length) or by added timing information from the SD.

synchronization to much better than 100 ns. This synchronization proves very powerful. Some simulation results are shown in Figure 3.

An important point is that only surface detector *times* are used in hybrid reconstruction. The SD densities are not used in determining the shower core position. Each density measurement is at a known core distance, unbiased by the density measurement itself. Moreover, since the SD densities do not

affect the hybrid geometry reconstruction, we are free to use the fluorescence-determined shower size at ground level as an independent cross-check of the shower size determined by the surface array alone.

The fluorescence reconstruction of the shower longitudinal profile follows the hybrid determination of the shower axis. The amount of light received by the eye determines the fluorescence light emitted as a function of depth along the shower axis, after correcting for distance to the shower, for the attenuation of light between the shower and the detector, and for the amount of Cherenkov light contaminating the signal. The fluorescence light emitted at the track is a measure of the total charged particle track length in a given depth bin. In this way, the shower development profile is reconstructed, and the shower energy and depth of maximum ($X_{\max}$) are determined (Dawson et al., 1996, 2001).

5   Simulation Results

5.1   Hybrid Aperture

The hybrid (fluorescence plus surface) triggering efficiency as a function of shower energy is shown in Figure 4(a). Even though the observatory is designed to be fully efficient only above 10^{19}eV, there is significant aperture available at lower energies, and those showers will be well reconstructed (see below).

Based on the AGASA energy spectrum (Takeda et al., 1998), this efficiency translates to a hybrid event rate at the south-

E	Δdirec.($^\circ$)		ΔCore(m)		ΔR_p(m)		$\Delta E/E$ (%)		$\Delta X_{\max}$(g cm^{-2})	
	50%	90%	50%	90%	50%	90%	50%	90%	50%	90%
10^{18}eV	0.50	1.55	35	155	20	97	9.5	20.5	21	74
10^{19}eV	0.35	1.10	35	120	16	76	4.5	12.5	14	62
10^{20}eV	0.35	0.90	30	100	13	64	2.5	16.5	12	69

Table 1. Summary of hybrid reconstruction resolution for a single Auger eye, for events with zenith angles $<60^\circ$ landing inside the array boundary. If more than one eye triggers on an event we use information from the eye with the longest angular track length. The detector is optimized for energies above 10^{19}eV but acceptable reconstruction is expected at energies down to 10^{18}eV. The values of the parameter bracketing 50% and 90% of the error distribution are given. The table lists errors in the arrival direction (i.e. space angle), core location, impact parameter, energy and depth of maximum.
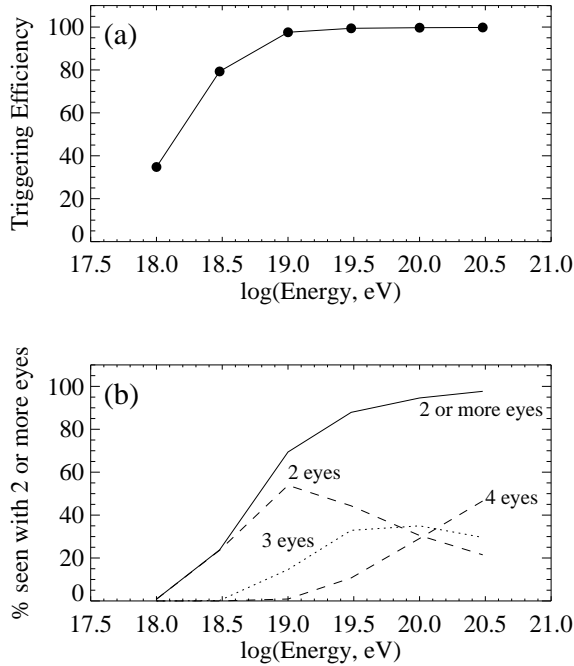
Fig. 4. (a) The hybrid triggering efficiency as a function of energy for showers (with zenith angles less than 60°) falling at random positions within the surface array boundary. At least one fluorescence eye and two surface detectors are required to trigger. The triggering aperture can be obtained by multiplying the efficiency by 7375 km^{2}sr. (b) The fraction of events triggering more than one fluorescence station.

ern site of 30,000 events per year above 10^{18}eV, 500 events per year above 10^{19}eV, and 10 events per year above 10^{20}eV. This assumes a 10% duty cycle for the FD and only includes showers with zenith angles smaller than 60°.

With four fluorescence sites the opportunity for stereo views of showers is very good, especially at higher energies. Figure 4(b) shows that at 10^{19}eV almost 70% of events will be seen by more than 1 fluorescence eye. Because we have access to surface array timing information, stereo views are not vital for geometrical reconstruction of the shower axis, but stereo views will greatly assist in cross-checks of our assumptions about atmospheric light attenuation. They will also allow us to empirically study our longitudinal profile

resolution without reliance on detector simulations.

5.2 Hybrid Reconstruction Precision

We have applied the hybrid reconstruction method to simulated air showers to arrive at the resolution figures shown in Table 1. No quality cuts have been applied to the data, and no "stereo" information has been used. When an event is viewed by more than one FD station, these simulations have used only information from the eye viewing the longest track length.

The table shows median errors and error values bracketing 90% of the data. Note that these are statistical errors only, and do not include systematic uncertainties connected with (for example) calibration or atmospheric transmission of light.

6 Conclusion

The hybrid detection of air showers is a hallmark of the Pierre Auger Observatory. It offers a large set of "gold-plated" events during the 10% of time when both fluorescence and surface detectors are operating. These events will have very well measured directions and energies, together with information on mass composition from both the FD and SD.

Just as importantly, hybrid shower measurements offer cross-checks and justification to the collaboration and to the community for the techniques that are used in analyzing the larger data set collected by the surface array alone.

References

Cester, R. for the Auger Collaboration, "The aperture, sensitivity and precision of the Auger fluorescence detector", HE1.8.4, these proceedings, 2001.

Dawson, B.R., Dai, H.Y., Sommers, P., and Yoshida, S., Astropart. Phys., 5, 239–247, 1996.

Dawson, B.R., Debes, M., and Sommers, P. "Shower Profile Reconstruction with Engineering Array FD Data", Pierre Auger Project Technical Note GAP-2001-016 (Fermilab, Batavia Illinois), 2001 (http://www.auger.org/admin)

Dova, M.T. for the Auger Collaboration, "Survey of the Pierre Auger Observatory", HE1.8.1, these proceedings, 2001.

Sommers, P., Astropart. Phys., 3, 349–360, 1995.

Takeda, M. et al., Phys. Rev. Lett., 81, 1163–1166, 1998.